REDUCED COMPLEXITY MODELING OF SHORELINE RESPONSE BEHIND OFFSHORE BREAKWATERS

Ahmed Elghandour[1,3,4,5], Dano Roelvink[1,2,3], Bas Huisman[2], Johan Reyns[1,2], Susana Costas[5] and Jaap Nienhuis[6]

Prediction of the shoreline response behind offshore breakwaters is essential for coastal protection projects. Due to the complexity of the processes behind the breakwaters (e.g., wave diffraction, currents, longshore transport), detailed modelling needs high computational efforts. Therefore, simplifying the process effect in a simpler coastline model could be efficient. In this study, the coastline evolution model ShorelineS is used. A new routine was implemented in the model to adjust the wave heights and angles behind the offshore breakwaters. Two approaches from the literature and a newly introduced one were tested in this study. The model free grid system was used to simply track the breaker line; such an advantage also helped to form tombolo, which is not common for these types of models. The tests showed promising results for single and multi breakwaters systems; however, the newly introduced approach still needs further testing and refinement for better performance and less computational cost.

Keywords: Coastline modelling; ShorelineS; wave diffraction

INTRODUCTION

Offshore breakwater schemes are applied as coastal protection measures in many places around the world. Predicting the response of the shoreline behind the breakwaters is, however, a great challenge for coastal engineers. Considerable changes in coastline curvature may take place behind the structure, especially when a tombolo develops. Detailed 2DH process-based models are often used to simulate the strongly curved local coastline features, but require an enormous computational effort to accurately compute the wave-driven transports. Using a coastline model would therefore be much more efficient, but the grids of the classical coastline models are typically not sufficiently flexible to cope with the curvature of tombolo's. The recently developed ShorelineS model (Roelvink et al., 2020) does, however, allow for flexible grid generation, which provides new opportunities. Here we add local wave shielding to the ShorelineS model to resolve the local coastline changes behind offshore breakwaters.

WAVE DIFFRACTION IN SHORELINE MODELS

In most of the existing shoreline models, the wave diffraction effect has been introduced; such a process should be simplified to avoid the high computational cost. Among the existing approaches; two were selected for this study: (the approaches are named by the studies first authors).

Dabees approach

The first selected approach was introduced by Dabees (2000). From the linear wave theory, to combine the refraction-diffraction behind the breakwaters, the wave heights are calculated as:

$$H = H_i K_r K_s K_d \qquad (1)$$

Where H_i is the incident wave height at the tip of the structure, K_r, K_s and K_d are refraction, shoaling, and diffraction coefficients, the latter can be obtained at any point behind the breakwater based on θ_{S-P} the angle between the shadow line and the point of interest P, as follows:

$$K_d = 0.69 + 0.008\theta_{S-P} \text{ for } 0 \geq \theta_{S-P} > -90 \qquad (2)$$

$$K_d = 0.70 + 0.37\sin\theta_{S-P} \text{ for } 40 \geq \theta_{S-P} > 0 \qquad (3)$$

$$K_d = 0.83 + 0.17\sin\theta_{S-P} \text{ for } 90 \geq \theta_{S-P} > 40 \qquad (4)$$

[1]Water science and Engineering Department, IHE Institute for Water Education, Westvest 7, Delft, 2611AX, the Netherlands
[2]Marine and Coastal systems, Deltares, Boussinesqweg 1, Delft, 2629 HV, the Netherlands
[3]Department of Hydraulic Engineering, Delft University of Technology, Stevinweg 1, Delft, 2628 CN, the Netherlands
[4]Department of Civil Engineering, Port Said University, Portfouad, Port Said, 42526, Egypt
[5]CIMA, University of Algarve, Campus de Gambelas, Faro, P-8005-139, Portugal
[6]Global Change Geomorphology, School of Geosciences, Utrecht University, Princetonlaan 8a, Utrecht, 3584 CB, the Netherlands

He introduced the concept of diffraction that starts from a source point I within a transitional distance 'G', that equals 2 to 3 times the wavelength. The distance from the breakwater to the source point (I):

$$X_1 = G(\frac{y}{s}) \tag{5}$$

The wave ray is assumed to follow a circular arc from the source point I to the point P, see Fig. 1-c.

$$\alpha_1 = (\theta_{IP} + \xi) \tag{6}$$

$$\alpha_P = (\theta_{IP} - \xi) \tag{7}$$

Where θ_{IP} is the angle of the straight line between I and P, α_1 is the starting angle at I, α_P is the wave angle at P, and ξ is the difference of the actual ray angle from the straight line angle. By applying Snell's law, where L_P and L_I are the wave lengths, then by substituting

$$\xi = \tan^{-1}\left[(\frac{L_I - L_p}{L_I + L_p}) \tan\theta_{IP} \right] \tag{8}$$

After calculating ξ, then α_I and α_P are obtained, finally the refraction coefficient K_r:

$$K_r = \sqrt{\frac{\cos\alpha_P}{\cos\alpha_1}} \tag{9}$$

Hurst approach

Hurst et al. (2015) developed a shoreline model to investigate the behaviour of crenulate-shaped bays exposed to differing directional wave climates. The technique they used is to modify the wave angle and the wave power that approaches the coast, using this simple rule

$$\theta_s = 1.5(|\omega - \theta_o|) \tag{10}$$

Where θ_s is the wave angle approached in the shadowed zone, ω is the angle between the shadow line and the shadowed cell and θ_o is the offshore wave approach angle.

WAVE DIFFRACTION IMPLEMENTATION IN SHORELINES

ShorelineS model computes shoreline changes behind offshore breakwaters as a result of the wave-driven transport. The computation of the effect of the breakwater on the breaking wave conditions (i.e., local wave height and angle) requires in the first place an accurate positioning of the breaker line, the methods to calculate these parameters are explained in this section.

Wave Height behind the Breakwater

For the wave height, Eq. 2,3, and 4 were used in the model. First, the K_d is calculated from each tip, before combine both:

$$K'^2 = K'^2_L + K'^2_R \tag{11}$$

where K' is the combined the diffraction coefficient, K'_L and K'_R are diffraction coefficients for the waves coming from left and right.

Wave angle treatment behind the breakwater

Several approaches for treating the wave angle behind the breakwater have been tested in this study; three main approaches are explained in this section. Fig. 3-a illustrates definitions of parameters used in this study.
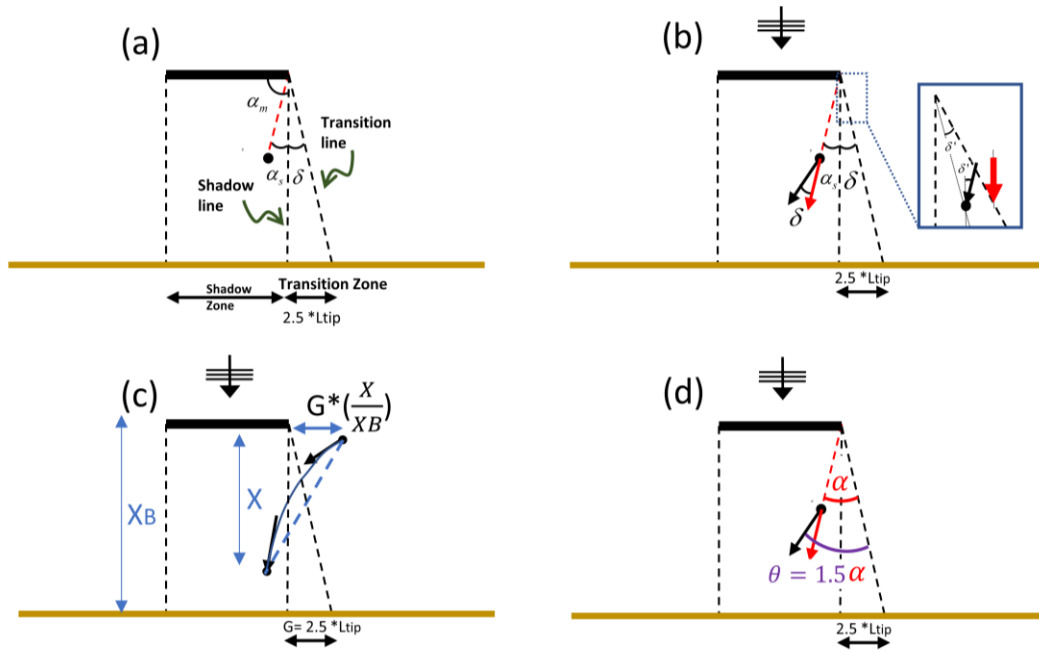
Figure 1. Definition sketch of (a) the parameters used in this study, (b) the new approach for the angle treatment behind the breakwater, (c) Dabees approach, and (d) modified Hurst approach.

1. Modified Hurst approach. Hurst approach (Hurst et al., 2015) was tested in this study after little modification: the diffracted wave angle is equal to 1.5 time the angle between the point of interest and the transition line (instead of the shadowed line). $\theta = 1.5(\delta + \alpha_s)$ Where θ is the diffracted wave angle measured from the transition line, see Fig. 3-d.

2. Dabees approach. The angles were calculated as explained before with no modification, see Fig. 3-c.

3. Roelvink approach. A new approach to treat the wave angle is introduced in this study. The approach estimates the wave angle in the sheltered zone using a relative changing rate, that lies between the two selected approaches from the literature, see Fig. 2. The approach divides the sheltered area into two zones: first, the transition zone, the angle changes from the offshore condition by adding the angle between the point of interest and the transition line δ' to the offshore wave angle. Second, within the shadowed zone, the angle between the point of interest and the transition line is measured $(\alpha_s + \delta)$, then it adds the angle δ (the angle between the shadow and the transition lines), so the new diffracted angle $\theta = (\alpha_s + 2\delta)$, see Fig. 3-b.

For all approaches, after calculating the diffracted angle from each tip; the final angle is combined based on the wave energy:

$$\theta = \tan^{-1}\left(\frac{H_L^{\,2} * \sin\theta_L + H_R^{\,2} * \sin\theta_R}{H_L^{\,2} * \cos\theta_L + H_R^{\,2} * \cos\theta_R} \right) \tag{12}$$

where θ', θ_R and θ_L are combined, right and left wave angles and H_L, H_R are Wave Heights from the left and right tips.
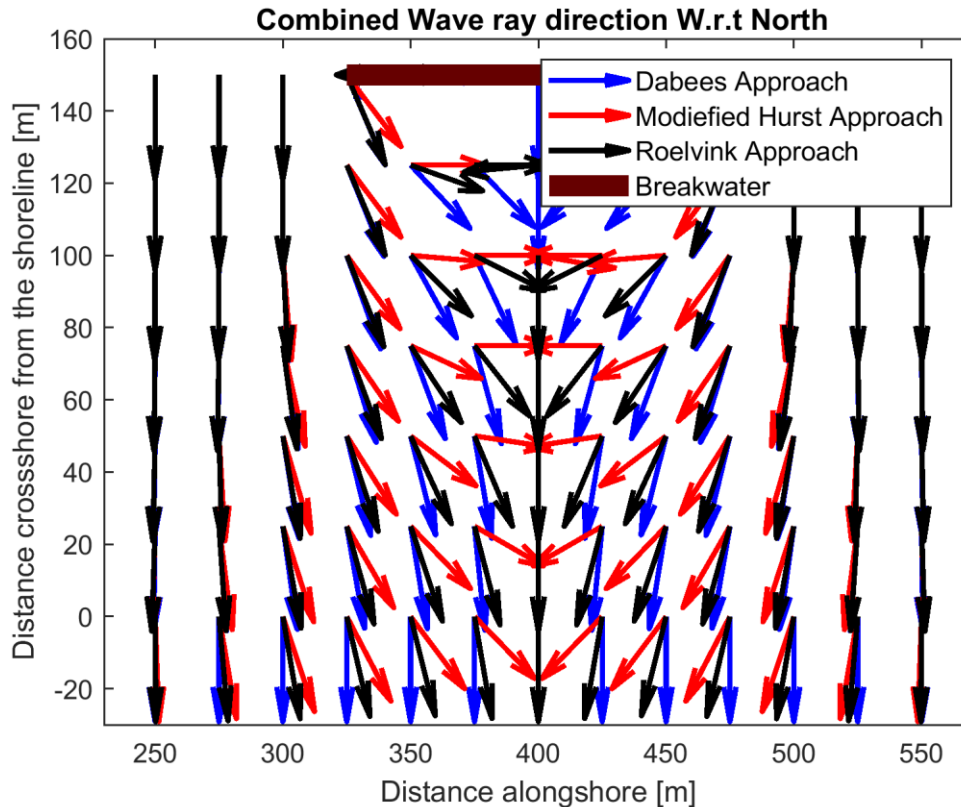
Figure 2. Computed wave shielding behind an offshore breakwater using three methods.

The breaker line behind the breakwater

   One of the challenges in simulating the shoreline response behind the breakwater using only longshore transport formulas is the position of the breaker line (where the model calculates the corrected values of the wave height and angles).

   In the existing models, it is common to assume a breaker line parallel to the shoreline, e.g., UNIBEST (Deltares, 2011).

   In this study, a new approach has been introduced, taking into account the advantage of the model's free grid system. The approach assumes one separate perpendicular profile for each segment of the shoreline, the profile length follows the well-known Dean profile. During the simulation, to determine the location of the breaker line points; first, based on the breaking wave heights, the model estimates the breaking depths, second, it calculates the distances to the breaking depths from the shoreline. Then, based on these locations, the wave coefficients are calculated to correct the breaking wave heights. Finally, based on the calculated height, the model repeats the calculation to better estimate the locations, see Fig. 3. One of the advantages of the free grid is that the breaking points are updated during the simulation as the shoreline position changes, see the red dots in Fig. 4-d, and Fig. 5. The wave heights behind the breakwaters are lower than outside; therefore, the breaking depth points should be closer to the shoreline.
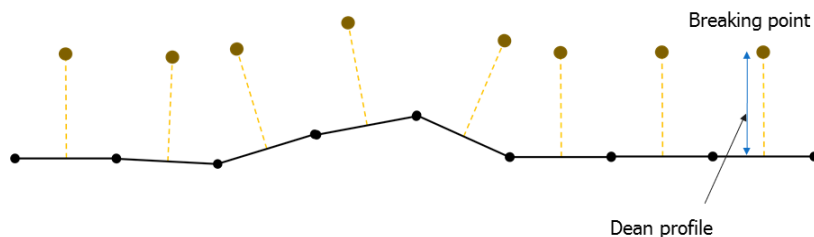
Figure 3. Definition sketch of the breaking line in ShorelineS.

VERIFICATION TESTS

The previous approaches were implemented in the model; then, they were tested through a verification test.

Verification criteria

Several studies have been done on the shoreline response behind the breakwater, to validate the model at this stage, two studies were chosen. First, a study by Hsu and Silvester (1990) who developed a dimensionless relationship for the salient formation based on analysing data from prototypes

$$\frac{x}{L_B} = 0.6784 \left(\frac{L_B}{X_B} \right)^{-1.1248} \tag{13}$$

Where L_B is the breakwater length, X_B is the distance between the breakwater and the original shoreline, and x is the distance between the new shoreline and the breakwater.

Second, a study by Khuong (2016) who used data for 93 projects with 1114 structures including physical conditions and shoreline measurements, and based on the analysis of such data, several empirical relationships were introduced regarding the salient or tombolo formation. For the salient, the study provided an empirical relation from the observation data:

$$\frac{x}{L_B} = 0.62 \left(\frac{L_B}{X_B} \right)^{-1.15} \tag{14}$$

For the tombolo formation behind a single breakwater, the study provided a criterion $L_B / X_B > 1$ which agrees with the laboratory study by Suh & Dalrymple (1987). Also, other empirical relations for tombolo width and the control points up and downdrift for the tombolo and salient formation were provided could be used to validate the model.

In this study, the above criteria were chosen for the test; in summary, the shoreline should build a tombolo if the ratio between the length to the distance is more than one. While if the ratio is less than one, the shoreline should form a salient that should match with the empirical formulas above.

To perform the test, each approach was examined by running the model on 12 different situations that expect to cover all possible responses: limited response, salient, or tombolo.

Different combinations of X_B and L_B were used to test the model for different expected responses, see Table 1.

Table 1. Twelve scenarios used in the test and their expected response.

XB/LB [m]	100	150	200	250
150	Salient	Salient/tombolo	tombolo	tombolo
200	Salient	Salient	Salient/tombolo	tombolo
250	Limited response	Salient	Salient	Salient/tombolo

Model setup

The test was performed nine times: the three wave angle approaches have been tested with three different methods to calculate the wave height (See Eq. 1) using $K_r K_s K_d$, $K_s K_d$ or K_d only.

The modified version of Kamphuis formula (Kamphuis, 1991), presented by Dabees (2000), was used in the test, to include the wave height gradients alongshore

$$Q_s = 2.33 H_{sb}^2 T^{1.5} m_b^{0.75} D_{50}^{-0.25} \left[\sin^{0.6} 2\phi_{locb} - \frac{2}{m_b} \cos \phi_{locb} \frac{dH_{sb}}{ds} \right] \tag{15}$$

The term $\frac{dH_{sb}}{ds}$ was implemented so at each point (i), the model calculates the difference in wave height between (i-1, i+1) then divided by the distance.

Other model inputs parameters were fixed for all simulations, see Table 2.

Table 2. Model input parameters.	
Parameter	Value
Mean wave direction	0°
Initial grid size	25 m
Wave Height	1.2 m
Wave peak period	7 sec
Closure Depth	10 m
Grain size	0.2 mm

Model result

For Dabees approach, the overall trend is matched with the empirical relations for the salient. However, it did not allow to form a tombolo, see Fig. 4-a. For the modified Hurst and Roelvink approaches, the trend is also matched with the salient and both were able to form a tombolo, except the case when wave heights are calculated using $K_r K_s K_d$, see Fig. 4-a and b. On the other hand using two coefficients $K_s K_d$ or K_d only, the results were acceptable, which has an advantage in terms of the simplicity of the calculations.
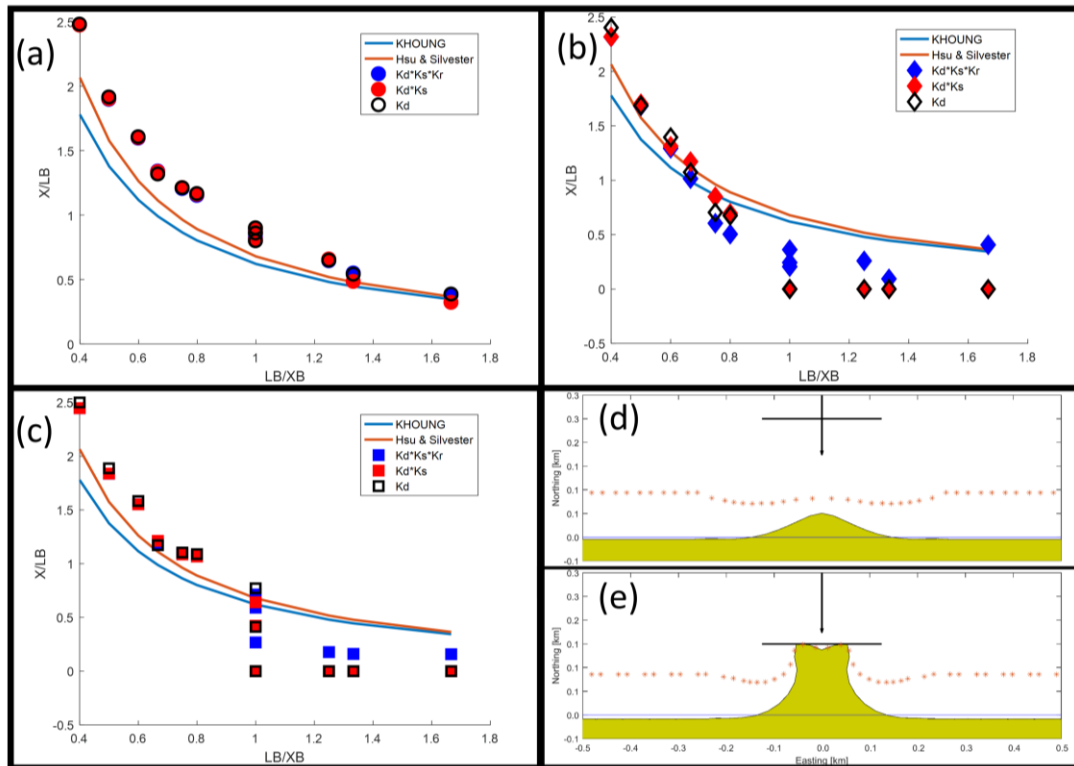

Figure 4. Verification tests results: (a) Dabees approach, (b) modified Hurst approach, (c) Roelvink approach; (d) Salient formation (length 250, distance 250), and (e) Tombolo formation (length 250, distance 150).

Generally, both approaches the modified Hurst and Roelvink were acceptable in terms of forming tombolo. From another perspective which is the model behaviour, the Roelvink approach was preferred as the tombolo formation was smoother than in Hurst simulation. For wave heights, the method with K_d was chosen for simplicity; see Fig. 4-d and e shows examples of salient and tombolo formation using Roelvink approach and only K_d , more test results can be seen in Elghandour (2018).

DISCUSSION AND CONCLUSIONS

Due to the offshore breakwater presence, the (breaking) wave height in the shadowed area is lower than in the exposed area. Such a difference leads to an alongshore gradient in the wave setup. Consequently, alongshore currents take place which leads to sand transport from the exposed to the shadowed area, so the equilibrium of the shoreline in the vicinity of the breakwater is mainly based on

the gradient in breaking wave height and wave setup (Heerdink, 2003). Therefore, the breaker depth gradient plays a role in the equilibrium shape of the shoreline.

To implement the previous concept into the model, a mechanism was introduced to track the breaker line throughout the calculation in the shielded area. Such mechanism enhances the estimation of the breaker depths which affect the values of the breaking wave height and the angle for each segment before substituting into the longshore transport formula.

Three different approaches were tested to determine the wave angles behind the breakwaters: two from the literature (Dabees, 2000; Hurst et al., 2015) with little modification and a new approach was introduced. The new approach and the modification to Hurst approach have no quantified physical interpretation. The main concept behind them is to gradually change the wave orientation from the exposed area to the shielded area behind the breakwater. Such approaches keep the model preferential advantage, which is simplicity by simplifying the phenomena without complex calculations.

In some situations, when the breakwater length is larger than the offshore distance, there is a chance for a tombolo formation. These chances increase for higher waves. Tombolo formation is not always the preferred shoreline response behind the breakwater. If the breakwaters are built to reduce the erosion, a tombolo formation might increase the erosion downdrift. Moreover, it can be dangerous for beach users if the breakwater is built on a recreational beach. Therefore, predicting the beach response is very important in such situations(Heerdink, 2003). The new approaches introduced to the model in this research showed the ability to simulate tombolo formation, which is not common for such type of simple models.

Although the new approaches show a better prediction of the response in terms of the ability to form tombolo, Dabees approach showed better matching with the empirical formulas. Using Dabees approach, the shoreline was not able to form a tombolo because of the treated wave angles. Roelvink approach showed better behaviour than the modified Hurst approach in salient/tombolo formation. A couple of disadvantages of the new approaches: first, the treated wave directions behind breakwaters fluctuate for the same configuration based on the waves condition, second the shoreline builds up behind the breakwater faster than usual. The factors used in the new approaches should be tuned by comparing to physical or 2/3D numerical models.

During the validation test, only the ratio between breakwater length to offshore distance was used to test the shoreline response; however, more than 14 variables affect the shoreline response according to Hanson and Kraus (1990). Another limitation of this study is testing the shoreline response only by the final distance to the breakwater, which ignores the configuration of the final plan form and the up/downdrift areas. Both limitations should be considered to validate the model either by real-world case studies or by comparing to more empirical relations introduced in Khuong (2016). In addition, the longshore transport formula that includes the tidal current, introduced by Hanson et al. (2006), should be considered in future work.

ACKNOWLEDGMENTS

REFERENCES

Dabees, M. (2000). *Efficient modeling of beach evolution. Ph.D. Thesis*. Civil engineering, Queen´s University, Kingston, Ontario, Canada.

Deltares. (2011). UNIBEST-CL+ Manual : Manual for version 7.1 of the shoreline model UNIBEST-CL+.

Elghandour, A. M. (2018). *Efficient Modelling of coastal evolution Development, verification and validation of ShorelineS model*. IHE Delft Insitute for Water Education, Delft, The Netherlands.

Hanson, H., & Kraus, N. C. (1990). Shoreline response to a single transmissive detached breakwater. *Coastal Engineering Proceedings*, *1*(22), 2034–2046. https://doi.org/10.9753/icce.v22.%p

Hanson, H., Larson, M., Kraus, N. C., & Gravens, M. (2006). Shoreline response to detached breakwaters and tidal current comparison of numerical and physical models. In *Coastal Engineering Proceedings* (pp. 3630–3642).

Heerdink, J. (2003). *Shoreline response to offshore breakwaters*. TU Delft. Retrieved from http://resolver.tudelft.nl/uuid:60adf444-6a18-4219-a84e-62500573638f

Hsu, J., & Silvester, R. (1990). Accretion behind single offshore breakwater. *Journal of Waterway, Port, Coastal, and Ocean Engineering*, *116*(3), 362–380. https://doi.org/10.1061/(ASCE)0733-950X(1990)116:3(362)

Hurst, M. D., Barkwith, A., Ellis, M. A., Thomas, C. W., & Murray, A. B. (2015). Exploring the
        sensitivities of crenulate bay shorelines to wave climates using a new vector-based one-line
        model. *Journal of Geophysical Research F: Earth Surface*, *120*(12), 2586–2608.
        https://doi.org/10.1002/2015JF003704

Kamphuis, J. W. (1991). Alongshore sediment transport rate. *Journal of Waterway, Port, Coastal, and
        Ocean Engineering*, *117*(6), 624–640. https://doi.org/10.1061/(ASCE)0733-
        950X(1991)117:6(624)

Khuong, T. C. (2016). *Shoreline response to detached breakwaters in prototype*. Delft University of
        Technology.

Roelvink, D., Huisman, B., Elghandour, A., Ghonim, M., & Reyns, J. (2020). Efficient modeling of
        complex sandy coastal evolution at monthly to century time scales. *Frontiers in Marine Science*,
        7, 535. https://doi.org/10.3389/fmars.2020.00535

Suh, K., & Dalrymple, R. a. (1987). Offshore Breakwaters in Laboratory and Field. *Journal of
        Waterway, Port, Coastal, and Ocean Engineering*, *113*(2), 105–121.
        https://doi.org/10.1061/(ASCE)0733-950X(1987)113:2(105)